

**Engineering Cation Vacancies in High-entropy Layered Double Hydroxides  
for Boosting Oxygen Evolution Reaction**

Junchuan Yao,<sup>a</sup> Fangqing Wang,<sup>a</sup> Wenjun He,<sup>a</sup> Ying Li,<sup>a</sup> Limin Liang,<sup>a</sup> Qiuyan  
Hao<sup>a,\*</sup> and Hui Liu<sup>a,\*</sup>

<sup>a</sup> Key Laboratory of Special Functional Materials for Ecological Environment and Information (Ministry of Education), Hebei University of Technology, Tianjin 300130, China

## **Experimental Section**

### **Materials.**

Ni(NO<sub>3</sub>)<sub>2</sub>·6H<sub>2</sub>O, Cu(NO<sub>3</sub>)<sub>2</sub>·3H<sub>2</sub>O and Zn(NO<sub>3</sub>)<sub>2</sub>·6H<sub>2</sub>O were purchased from Aladdin, Fe(NO<sub>3</sub>)<sub>3</sub>·9H<sub>2</sub>O and Co(NO<sub>3</sub>)<sub>2</sub>·6H<sub>2</sub>O were purchased from Innochem, NH<sub>4</sub>F was purchased from Fuchen (Tianjin) Chemical Reagent Co., Ltd. (China), Urea was purchased from Tianjin City Guang Fu Tech. Development Co., Ltd. (China), KOH and ethanol were purchased from Tianjin Fengchuan Chemical Reagent Co., Ltd. (China). All the reagents were analytical grade and used after purchase without further purification. Deionized water (18.2 MΩ·cm) was self-made in the laboratory.

### **Synthesis of HE-LDHs/CC.**

First, the carbon cloth (CC) was cleaned with deionized water, ethanol and 0.1 M H<sub>2</sub>SO<sub>4</sub> aqueous solution. Second, 0.182 g of Fe(NO<sub>3</sub>)<sub>3</sub>·9H<sub>2</sub>O (0.45 mmol), 0.131 g of Co(NO<sub>3</sub>)<sub>2</sub>·6H<sub>2</sub>O (0.45 mmol), 0.131 g of Ni(NO<sub>3</sub>)<sub>2</sub>·6H<sub>2</sub>O (0.45 mmol), 0.109 g of Cu(NO<sub>3</sub>)<sub>2</sub>·3H<sub>2</sub>O (0.45 mmol), 0.134 g of Zn(NO<sub>3</sub>)<sub>2</sub>·6H<sub>2</sub>O (0.45 mmol), 0.148 g of NH<sub>4</sub>F (4 mmol) and 0.6 g of urea (10 mmol) were dissolved in 35mL deionized water to form a homogeneous solution. The above solution and one piece of carbon cloths (1 × 3 cm<sup>2</sup>) were transferred into a Teflon autoclave and then was heated for 6 h at 120 °C in a drying oven. After naturally cooled to room temperature, the sample was taken out and cleaned with deionized water. Finally, the HE-LDHs/CC was obtained after dried at 60 °C for 12 h in a vacuum dryer.

### **Synthesis of HE-LDHs-V<sup>+</sup>/CC.**

First, one piece of HE-LDHs/CC was immersed in a 2M KOH aqueous solution and stirred lightly for 30 min at room temperature. The HE-LDHs-V<sup>+</sup>/CC was obtained after cleaned with deionized water and dried at 60 °C for 12 h in a vacuum dryer.

### **Synthesis of NiFe-LDHs/CC.**

NiFe-LDH/CC was synthesized using the hydrothermal method under the same conditions as the synthesis of HE-LDHs/CC. For rational comparison, the total molar amount of metal nitrates (2.25 mmol) and the M<sup>2+</sup>/M<sup>3+</sup> molar ratio (4) in the synthesis solution were controlled to be constant. Therefore, 0.524 g of Ni(NO<sub>3</sub>)<sub>2</sub>·6H<sub>2</sub>O (1.8 mmol) and 0.182 g of Fe(NO<sub>3</sub>)<sub>3</sub>·9H<sub>2</sub>O (0.45 mmol) were added to the synthesis

solution.

### **Characterization.**

X-ray diffraction (XRD) patterns were measured with a RIGAKU SmartLab with Cu K $\alpha$  radiation ( $\lambda = 1.5418 \text{ \AA}$ ). Scanning electron microscope (SEM) images were taken on a Quanta 450 FEG. Transmission electron microscopy (TEM) images, high-resolution TEM (HRTEM) images and the corresponding energy dispersive spectroscopy (EDS) results were carried out on a JEM 2100F. The X-ray photoelectron spectroscopy (XPS) was performed on Thermo ESCALAB 250XI. Electron paramagnetic resonance (EPR) was measured by Bruker EMXplus. Raman spectra was taken on a LabRAM HR Evolution. Inductively coupled plasma-Mass Spectrometry (ICP-MS) was performed on Agilent ICP-MS 7800.

### **Electrochemical measurements.**

All electrochemical tests were done on the CHI660E electrochemical workstation using a typical three-electrode system in which a graphite rod was used as the counter electrode and a standard Hg/HgO was used as the reference electrode. The samples loaded with carbon cloth were cut into pieces ( $1 \times 1 \text{ cm}^2$ ) to serve as working electrodes. All the measurements were carried out in 1 M KOH at room temperature. Potentials in this work were all referred to the reversible hydrogen electrode (RHE) through the Nernst equation as follows:  $E \text{ (vs. RHE)} = E \text{ (vs. Hg/HgO)} + 0.099 + 0.0591 \times \text{pH}$ . Polarization curves were obtained by linear sweep voltammetry (LSV) at a scan rate of 2 mV/s with 90% i-R compensation. The Tafel slope was obtained from the polarization curves according to the equation:  $\eta = a + b \log |j|$ , in which  $\eta$  is the overpotential,  $b$  is the Tafel slope, and  $j$  is the current density. The double-layer capacitance ( $C_{dl}$ ) was obtained by cyclic voltammetry (CV) method processing in the non-Faradaic region at different scan rates and the electrochemically active surface areas (ECSA) were derived from the  $C_{dl}$ . The electrochemical impedance spectroscopic (EIS) tests were carried out from 100 kHz to 0.01 Hz at 1.38 V (vs. RHE). The electrochemical stability of the sample was evaluated by I-t curves from the Chronoamperometry (CA) method.

### **DFT Calculations.**

Density functional theory (DFT) calculations were performed using the Vienna

Ab initio Simulation Package (VASP).<sup>1</sup> Electron exchange and correlation interactions were described using a generalized gradient approximation (GGA) with a Perdew-Burke-Ernzerhof (PBE) functional.<sup>2</sup> The  $3 \times 3 \times 1$  Monkhorst-Pack sampling of the Brillouin zone is used for integration and the cutoff energy was 450 eV. Geometric optimization was performed using the conjugate gradient method with convergence thresholds set at  $10^{-5}$  eV for energy and  $0.02 \text{ eV \AA}^{-1}$  for force. The crystal plane of HE-OOH and HE-OOH- $V^+$  used is the (110) plane, and the vacuum layer was 15 Å. The geometric parameters of the supercell model are  $a= 10.59650 \text{ \AA}$ ,  $b= 13.90840 \text{ \AA}$ ,  $c= 16.26070 \text{ \AA}$ .

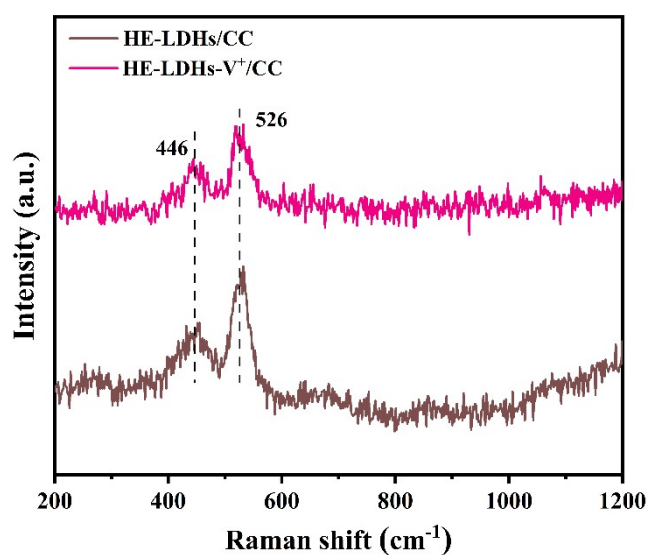


**Fig. S1.** Raman spectra of HE-LDHs/CC and HE-LDHs- $V^+$ /CC.

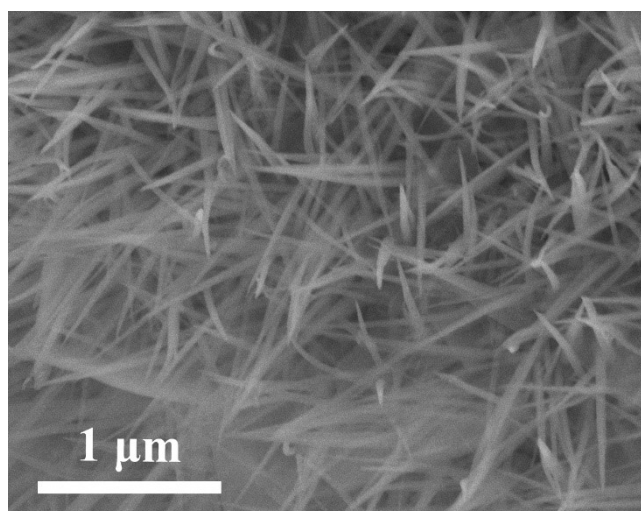


**Fig. S2.** SEM image of HE-LDHs/CC.

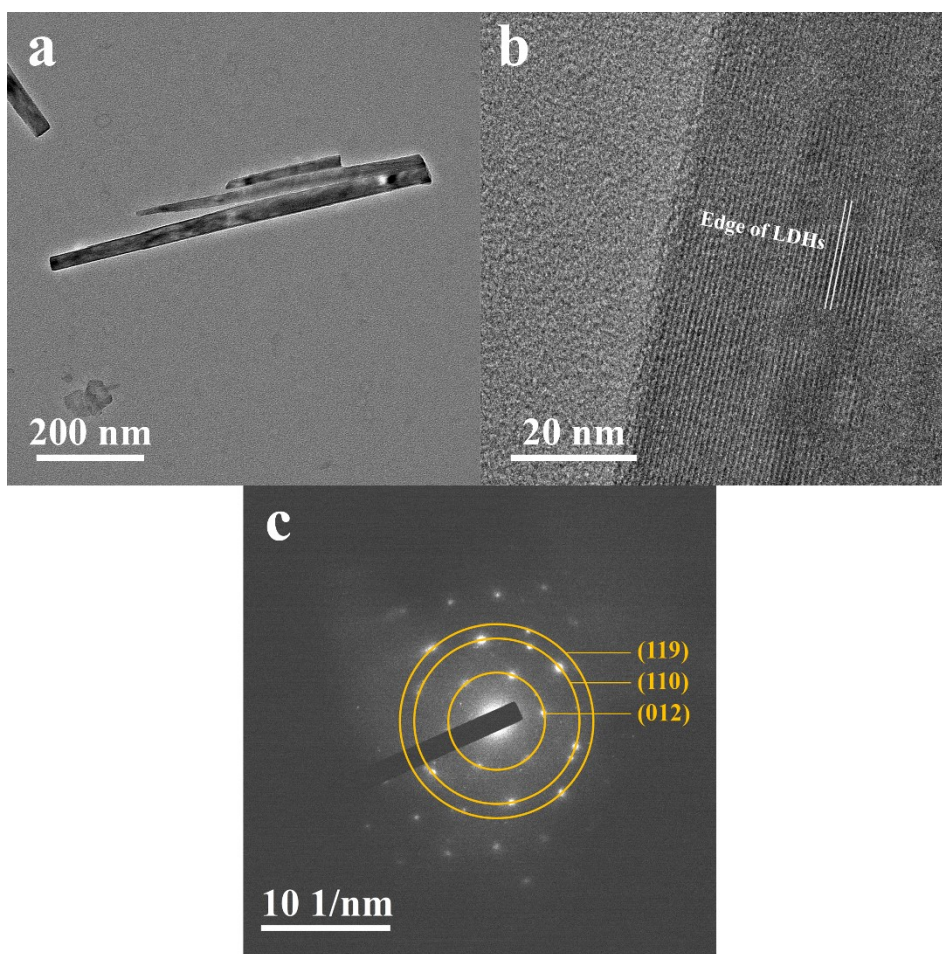


**Fig. S3.** (a) TEM image, (b) HR-TEM image and (c) SAED pattern of HE-LDHs.

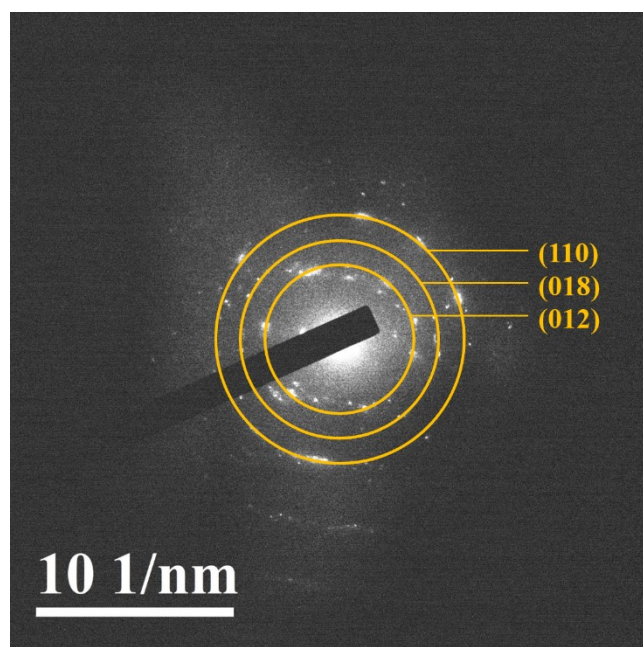


**Fig. S4.** SAED pattern of HE-LDHs-V<sup>+</sup>.

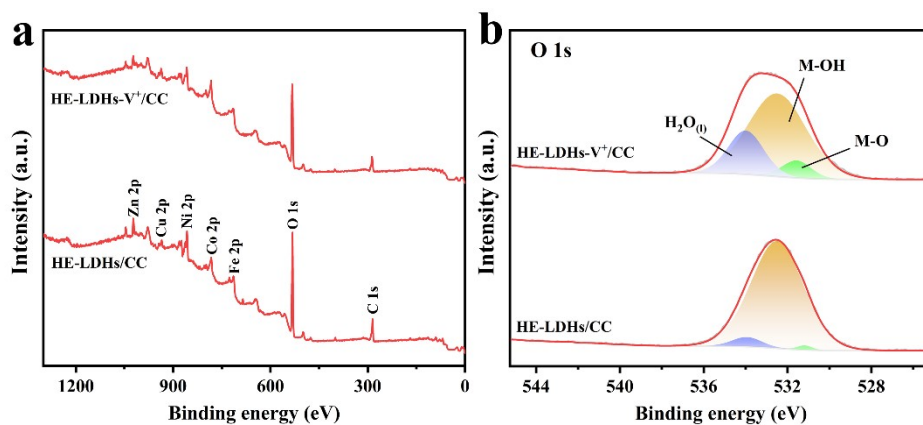


**Fig. S5.** (a) XPS survey spectra of HE-LDHs/CC and HE-LDHs-V<sup>+</sup>/CC. (b) O 1s XPS spectra of HE-LDHs/CC and HE-LDHs-V<sup>+</sup>/CC.

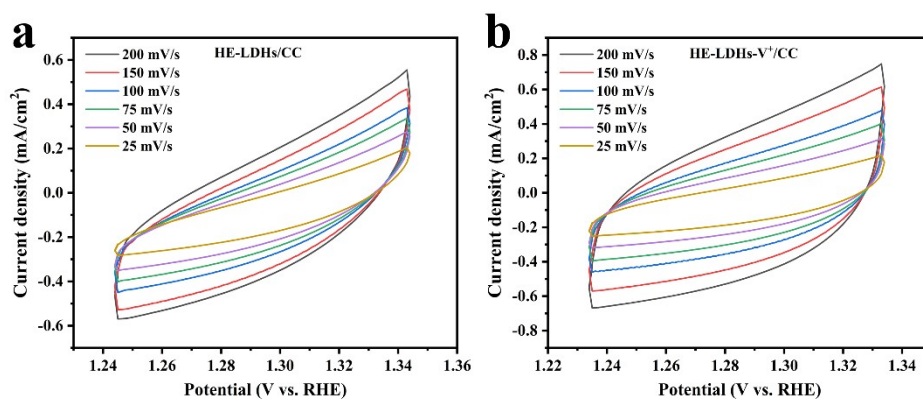


**Fig. S6.** CV curves of (a) HE-LDHs/CC and (b) HE-LDHs-V<sup>+</sup>/CC with scan rates from 25 mV/s to 200 mV/s.

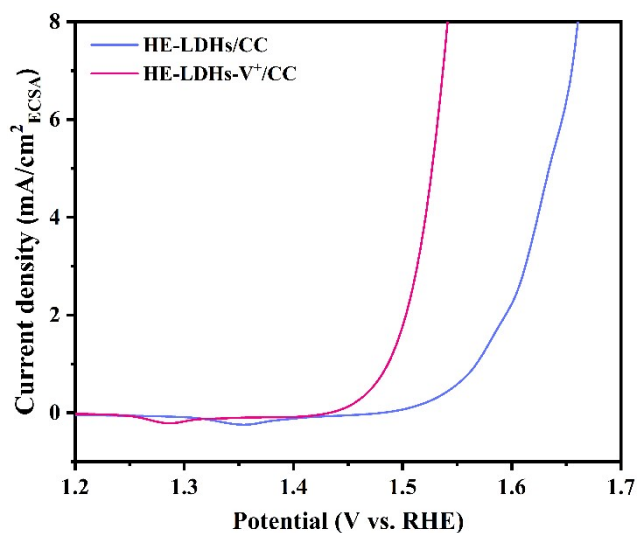


**Fig. S7.** Specific activity of HE-LDHs/CC and HE-LDHs-V<sup>+</sup>/CC based on ECSA.

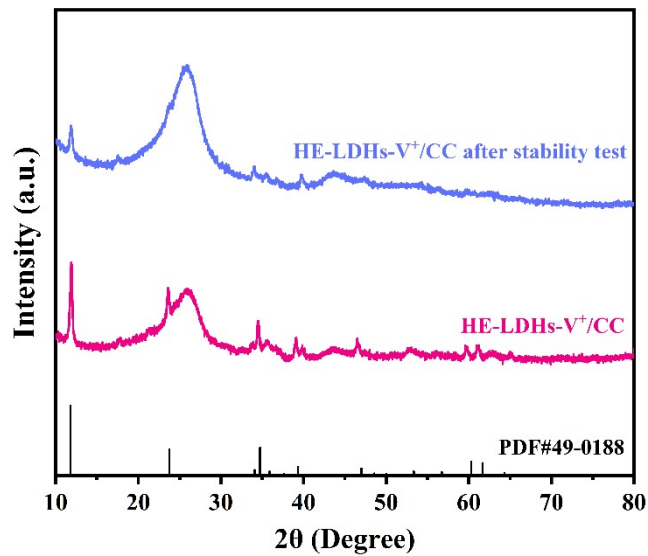


**Fig. S8.** XRD patterns of HE-LDHs-V<sup>+</sup>/CC and HE-LDHs-V<sup>+</sup>/CC after stability test.

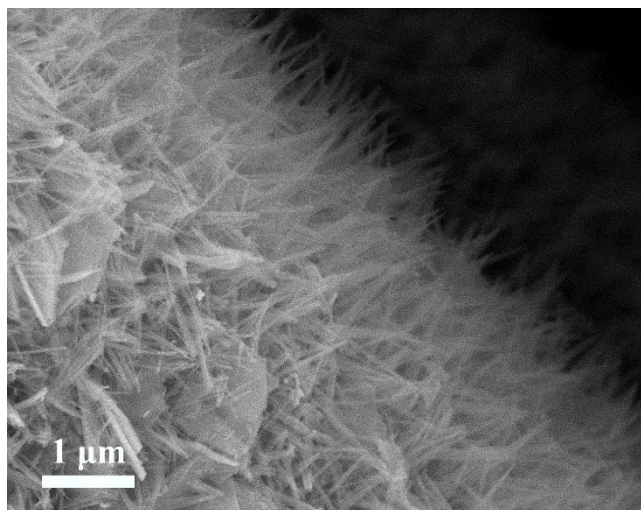


**Fig. S9.** SEM image of HE-LDHs-V<sup>+</sup>/CC after stability test.

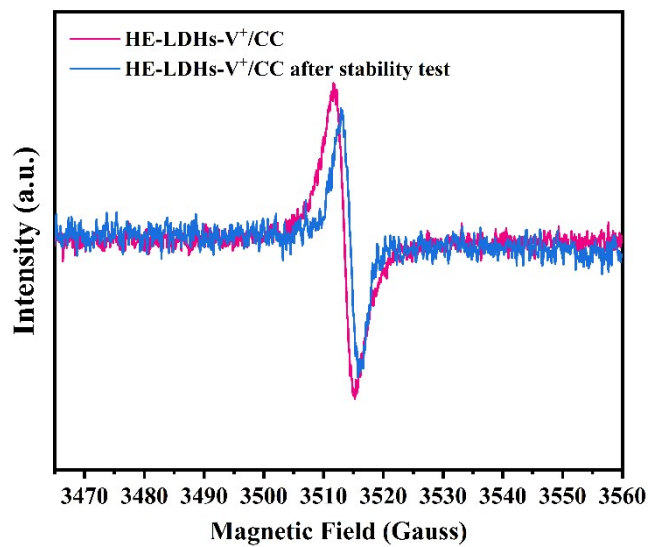


**Fig. S10.** EPR results for HE-LDHs-V<sup>+</sup>/CC and HE-LDHs-V<sup>+</sup>/CC after stability test.

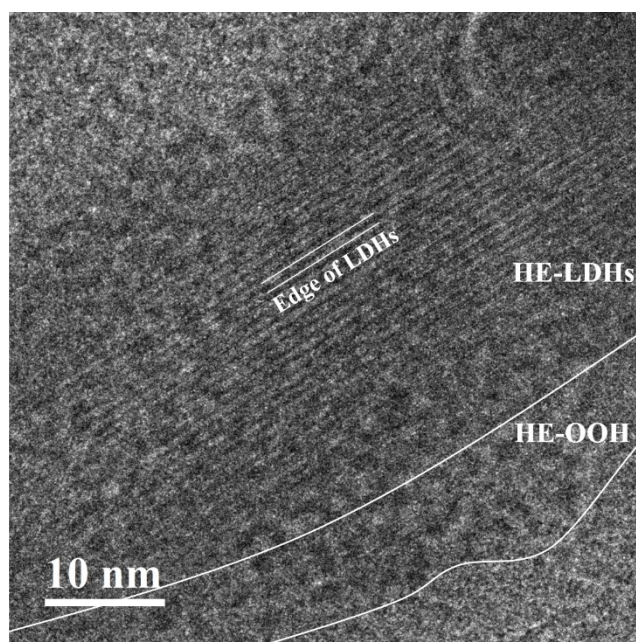


**Fig. S11.** HR-TEM image of HE-LDHs-V<sup>+</sup> after stability test.

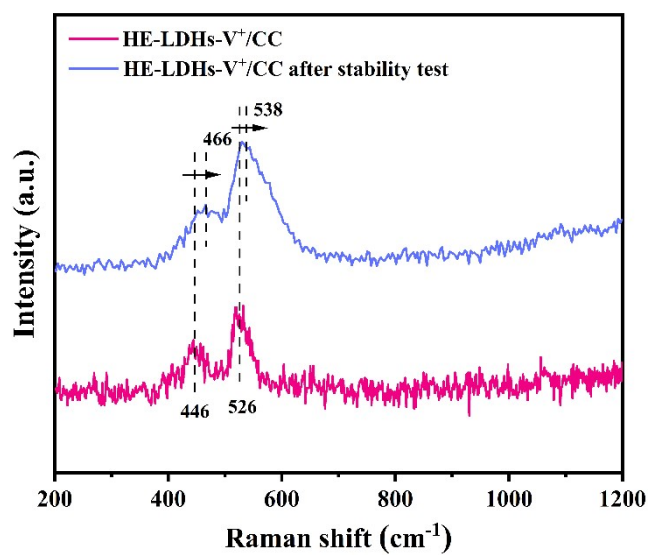


**Fig. S12.** Raman spectra of HE-LDHs-V<sup>+</sup>/CC and HE-LDHs-V<sup>+</sup>/CC after stability test.



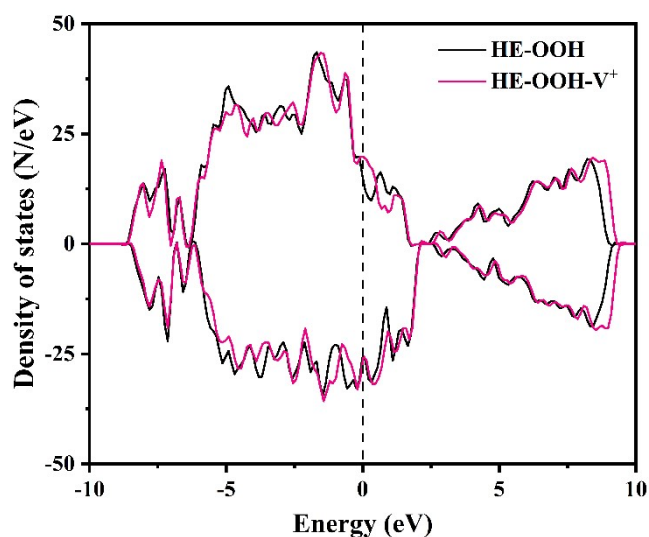


**Fig. S13.** TDOS plots of HE-OOH and HE-OOH-V<sup>+</sup>.

**Table S1.** ICP-MS results of chemical etching solutions and electrolyte after stability

Sample	test				
	Concentration (ppm)				
	Fe	Co	Ni	Cu	Zn
Chemical etching solutions	0.056	0.051	0.026	0.941	0.215
Electrolyte after stability test	0.024	0.008	0.014	0.013	0.017

**Table S2.** EDS results of HE-LDHs and HE-LDHs-V<sup>+</sup>

Sample	Elements content (At. %)					
	Fe	Co	Ni	Cu	Zn	O
HE-LDHs	1.21	10.63	6.90	4.85	2.14	74.27
HE-LDHs-V <sup>+</sup>	1.13	11.59	8.19	4.52	2.08	72.49

## Reference

1. Y. Cheng, L. Wang, Y. Song and Y. Zhang, *J. Mater. Chem. A*, 2019, **7**, 15862-

15870.

2. S. Zhao, C. Tan, C.-T. He, P. An, F. Xie, S. Jiang, Y. Zhu, K.-H. Wu, B. Zhang, H. Li, J. Zhang, Y. Chen, S. Liu, J. Dong and Z. Tang, *Nat. Energy*, 2020, **5**, 881-890.